

Contents lists available at ScienceDirect

Water Research

journal homepage: www.elsevier.com/locate/watres





Wildfire impact on disinfection byproduct precursor loading in mountain streams and rivers

Kenneth Hickenbottom, Krishna Pagilla, David Hanigan

Department of Civil and Environmental Engineering, University of Nevada, 1664 N Virginia St, Reno, NV 89557, United States

ARTICLE INFO

Keywords:
Pyrogenic organic matter
Haloacetonitriles
Haloacetamides
Nitrogenous DBPs
Trihalomethanes

ABSTRACT

We investigated short (first post-fire precipitation)- and long-term (11-month) impacts of the Caldor and Mosquito Fires (2021 and 2022) on water quality, dissolved organic matter, and disinfection byproduct (DBP) precursors in burned and adjacent unburned watersheds. Both burned watersheds experienced water quality degradation compared to their paired unburned watersheds, including increases in dissolved organic carbon (DOC), dissolved organic nitrogen (DON), and DBP precursors from precipitation events. DBP precursor concentrations during storm events were greater in the Caldor Fire's burned watershed than in the unburned watershed; precursors of trihalomethanes (THMs), haloacetic acids (HAAs), haloacetonitriles (HANs), and haloacetamides (HAMs) were 533 μ g/L, 1,231 μ g/L, 64 and 58 μ g/L greater. The burned watershed of the Mosquito Fire also had greater median concentrations of THM (44 µg/L), HAA (37 µg/L), HAN (7 µg/L), and HAM (13 µg/L) L) precursors compared to the unburned watershed during a storm immediately following the fire. Initial flushes from both burned watersheds formed greater concentrations of more toxic DBPs, such as HANs and HAMs. The Caldor Fire burn area experienced a rain-on-snow event shortly after the fire which produced the greatest degradation of water quality of all seasons/precipitation events/watersheds studied. Over the long term, statistical analysis revealed that DOC and DON values in the burned watershed of the Caldor Fire remained higher than the unburned control (0.98 mg C/L and 0.028 mg N/L, respectively). These short and long-term findings indicate that wildfires present potential treatment challenges for public water systems outside of the two studied

1. Introduction

Forested catchments are important sources of drinking water, serving as sources of water for two-thirds of municipalities, and at least partially contributing to the water supply of ~150 million people in the U.S. (Bladon et al., 2014; Liu et al., 2021). Wildfires in forested catchments have increased in frequency and size during the past several decades due to earlier spring onset, increased drought, higher temperature, and increased fuel aridity (Emelko et al., 2011; Westerling et al., 2006; Abatzoglou and Williams, 2016). These trends are the most significant in montane regions, such as the Sierra Nevada, Cascade, and Rocky Mountain ranges in the western US (Dennison et al., 2014). Wildfire is known to impact water quality and can change soil physical properties

by volatilizing carbon and other nutrients and increasing soil hydrophobicity, which can contribute to erosion (Certini, 2005; Beyers et al., 2005; Doerr et al., 2000). Affected forests experience higher erosion rates, which increases downstream sediment and nutrient loading and can affect drinking water quality by degrading raw water quality (Cawley et al., 2017; Sanchez et al., 2014; Smith et al., 2011).

Wildfires also modify soil-derived dissolved organic matter (DOM) characteristics (Fernández et al., 1997; Knicker et al., 2005; Podgorski et al., 2012; Thurman et al., 2020). Wildfire-affected DOM in runoff has increased concentrations and diversity of aromatic compounds, which are important precursors for disinfection byproducts (DBPs) in drinking water (Hohner et al., 2019; Le Roux et al., 2016; Linge et al., 2020). DBPs are formed when disinfectants such as chlorine or chloramines are

Abbreviations: BIF, Bromine Incorporation Factor; C-DBP, Carbonaceous Disinfection Byproduct; DBP, Disinfection Byproduct; DIN, Dissolved Inorganic Nitrogen; DOM, Dissolved Organic Matter; DON, Dissolved Organic Nitrogen; FI, Fluorescence Index; HAA, Haloacetic Acid; HAN, Haloacetonitrile; HAM, Haloacetamide; N-DBP, Nitrogenous Disinfection Byproduct; SUVA₂₅₄, Specific Ultraviolet Absorbance at 254nm; TOC, Total Organic Carbon; TDN, Total Dissolved Nitrogen; TP, Total Phosphorus; TTHM, Total Trihalomethane; THM, Trihalomethane; UFC, Uniform Formation Conditions; USEPA, US Environmental Protection Agency.

E-mail address: dhanigan@unr.edu (D. Hanigan).

^{*} Corresponding author.

added to reduce pathogenic risk to produce safe drinking water. Some DBPs are carcinogens or teratogens, which pose a risk to public health (Wagner and Plewa, 2017). Two subsets of carbonaceous DBPs (C-DBPs), trihalomethanes (THMs) and haloacetic acids (HAAs), have been demonstrated to be the largest classes of DBPs formed in drinking water treatment plants (Krasner et al., 2006) and are regulated by the US Environmental Protection Agency (USEPA, 2006) and the European Union (The European Parliament and the Council of the European Union, 2020). Other subsets of DBPs, including nitrogenous DBPs (N-DBPs) such as haloacetonitriles (HANs), haloacetamides (HAMs), and halonitromethanes, are not yet regulated but are thought to be substantially more cytotoxic and genotoxic to humans than C-DBPs (Bond et al., 2011; Komaki et al., 2014; Richardson et al., 2007; Wagner and Plewa, 2017). Because fire alters DOM characteristics and its concentration in runoff, the DBP precursors present downstream from a wildfire are thought to be substantially different and present at different concentrations than those from unaffected areas. For example, increased DOM concentrations have been linked to higher THM and HAA formation in runoff from burned catchments (Revchuk and Suffet, 2013; Uzun et al., 2020). Furthermore, watersheds with as little as 10% of their surface area affected by wildfire had higher DBP vields on a carbon-normalized basis when compared to other unburned watersheds (Writer et al., 2014).

Though there have been prior reports of water quality and DBP formation after wildfire, the existing body of research focuses primarily on experiments conducted at bench scale with soil leachate or limited surface water sampling campaigns (Cawley et al., 2017; H. Chen et al., 2020; Hohner et al., 2016; Revchuk and Suffet, 2013; Uzun et al., 2020; Writer et al., 2014). Of the published body of literature, three studies have focused on forest-scale surface water quality effects post-wildfire. These studies demonstrated increased C- and N-DBP precursor loadings in the year following wildfire, especially during rainstorms and spring snowmelt, compared to both pre-fire concentrations and concentrations in unburned catchments (Hohner et al., 2016; Uzun et al., 2020; Writer et al., 2014). Writer et al. (2014) found that DOC-normalized DBP yields during rainstorms and snowmelt in specific Colorado watersheds were significantly higher than yields outside of precipitation/snowmelt of the five EPA-regulated HAAs (HAA5) and four commonly measured HANs (HAN4). Hohner et al. (2016) also showed total THM (TTHM), HAA5, and HAN4 carbon-normalized yields were higher post-rainstorm in the Cache Le Poudre watershed (Colorado, USA) following wildfire. Increased dissolved organic nitrogen (DON) concentrations following rainstorms were associated with increased N-DBP formation potential (Hohner et al., 2016). Contrarily, Uzun et al. (2020) found that TTHM and HAA5 yields were not significantly affected by wildfire in two different Northern California watersheds characterized by moderate burn severity. They did not investigate HANs and HAMs. Both publications also reported changes in DOM characteristics; Uzun et al. (2020) reported increased specific ultraviolet absorbance (SUVA) during rain events post-wildfire when compared to reference watersheds, while Hohner et al. (2016) and Writer et al. (2014) found no significant difference in spring runoff or baseflow conditions compared to reference watersheds. Laboratory studies have noted increased SUVA₂₅₄ values in thermally altered organic matter over controls, indicating that the difference between surface water sampling may be due to precipitation events flushing pyrogenic DOM into surface water (Cawley et al., 2017; McKay et al., 2020; Wang et al., 2015). Overall, the limited number of studies focusing on forest-scale water quality data post-wildfire, and the limited number of samples leads to some conflicting conclusions. Further, there are no existing data on HAM formation post-wildfire, and when HANs have been measured, only 4 out of a possible 6 HANs were quantified. Finally, there has been recent EPA interest in regulating nine HAAs (HAA9), rather than the currently regulated five (HAA₅), and the available body of literature does not contain data or conclusions related to the additional four HAAs (Samson and Seidel, 2022).

Our objective was to address knowledge gaps pertaining to changes in DOM reactivity in forming relevant regulated and unregulated DBPs and water quality at the forest/catchment scale in multiple surface waters after two wildfires. To achieve this objective, we conducted high-frequency sampling of streams in adjacent burned and unburned watersheds after the Caldor Fire (2021, California, USA) and the Mosquito Fire (2022, California, USA). We measured DBP formation potential and various aspects of water quality during first-flush runoff events in both watersheds immediately post-wildfire. Additionally, for the Caldor Fire, we collected and analyzed samples to understand the long-term effects up to 11 months following the fire. The results have implications for public water drinking supplies affected by wildfire.

2. Methods and materials

2.1. Study sites and sampling

Burned and unburned watersheds were sampled from two fires in the Sierra Nevada Mountains of California, USA; the Caldor Fire (August-October 2021) and Mosquito Fire (September-October 2022). The Sierra Nevada is characterized by a Mediterranean climate with cool, wet winters and warm to hot summers. Vegetation between the two fires varies: the Caldor Fire study watershed is characterized by mixed pine and subalpine mixed conifer forests, while the Mosquito Fire study watershed contained oak woodlands, mixed oak/conifer woodlands, and mixed conifer forests (Dahlgren et al., 1997). These study sites were deemed comparable due to their location in the same mountain range and the similar ecological and climactic profiles of the upstream watersheds.

Caldor Fire sampling sites were in the Lake Tahoe Basin, within the Cold Creek and Trout Creek watersheds. In the Trout Creek watershed, 13% was unburned or very low severity, 39% was low severity, 45% was moderate severity, and 3% was high severity burn area (Ellsworth and Stamer, 2021). The Cold Creek watershed contained only a small portion of unburned to very-low severity burn area, with the majority of the watershed being unburned (Fig. 1& SI-1). Twenty-three 900 mL composite samples (300 mL every 30 min) were collected from Cold Creek over 36 h on October 5-7th, 2021, and from Trout Creek on October 17-19th, 22-23rd, and 24-25th, 2021 following two storm systems and based on the availability of forest access and closures imposed by the US Forest Service. At the time the study began, only one autosampler was available for use, limiting the ability to study the response of burned and unburned creeks from storms concurrently. The first sampling event from Cold Creek was meant to provide baseline conditions of an unburned creek in the area. 900 mL composite samples (300 mL every 40 min) were also taken during the month of December 2021 to capture runoff from major storms impacting the burn area. December storms are likelier to produce snow and thus very little runoff, instances of shifting polar to tropical airmasses have been known to occur in the Sierra Nevada Mountains, which can produce rain-on-snow events and large amounts of runoff (National Oceanic and Atmospheric Administration 1997). 900 mL grab samples were also taken at 3pm daily from January-September 2022. All samples were collected with a Teledyne ISCO 6712 Autosampler, except grab samples from Cold Creek from April-September 2022. Samples were retrieved from the ISCO samplers every 7 days and placed on ice for transport to the Harry Reid Engineering Laboratory at the University of Nevada, Reno for analysis. Changes in chemical and physical characteristics of water samples are subject to occur during storage, handling, and processing. However, Allen-Diez et al. (1998) noted no significant water quality changes in unfiltered samples from the Sierra Nevada Mountains stored at room temperature for 7 days, though small significant changes to pH, NH₄⁺, $\mathrm{NO_3^-}$ in samples from alpine/subalpine lakes have been noted after 48 h (Korfmacher and Musselman, 2007). To mitigate the effects of warm temperatures on sample storage, autosamplers were placed out of direct sunlight and the sampling chamber was always noted to be 15-20 °C,

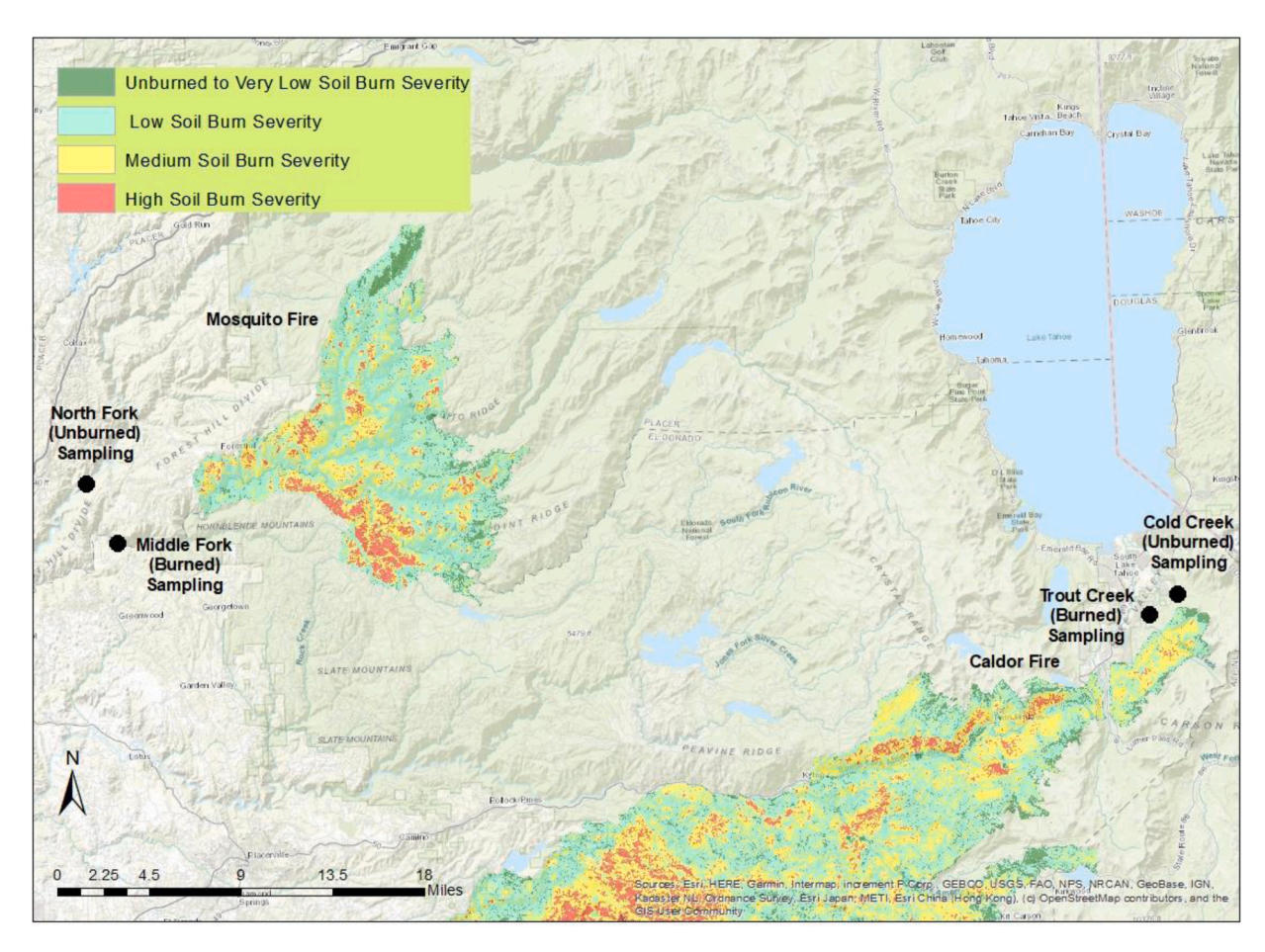


Fig. 1. Overview map over the Caldor and Mosquito Fire Study Site. Detailed maps of the study areas can be found in Figs. SI-1 and SI-2.

even during summer months at both study sites. The average nighttime temperature during the Mosquito Fire sampling was $12\,^{\circ}\mathrm{C}$ and $5\,^{\circ}\mathrm{C}$ from May 1 to September 20, 2022, during the Caldor Fire sampling. Based on this, we do not expect that water constituents were substantially changed during the storage period. Further, samples taken first were stored on-site in the sampler for longer than the last sample drawn, and therefore any changes would be observable as a systematic error occurring in the earlier samples of each 24-sample set. No such systematic error was observed (regression between time in sampler and various constituents).

Storms affecting the Caldor Fire burn area were mixed rain and snow and occurred on October 5, 17–18, 21–22, and 24–25, 2021. The bulk of the precipitation captured by the automated sampling occurred on October 24th and 25th, 2021, and began as a rain-on-snow event, followed by deposition of >0.6 m of snow. The intensity of this storm caused the autosampler to be inadvertently inclined due to soil subsidence beneath the sampler. As a result, only 10 samples were recovered during this sampling period. These samples incidentally aligned with peak runoff and a portion of the declining runoff, as measured by the United States Geological Survey Trout Creek monitoring station, located 3.6 km downstream of the Trout Creek sampling location. From December 24th to 30th, 2021 another large storm resulted in the deposition of ~5.5 m of snow. The following months of sampling had limited smaller storms and precipitation.

The Mosquito Fire (September-October 2022) affected communities in the Sierra Nevada foothills east of Sacramento, CA, and burned a large portion of the watershed of the Middle Fork of the American River. Burn severity was 7% unburned, 58% low severity, 25% moderate severity, and 9% high severity burn area (Figs. 1& SI-2). The North Fork of the American River was little affected, with only 4% and $<\!1\%$ of the two

contributing sub-watersheds being burned (Mosquito Fire BAER, 2022). A precipitation event occurred in the burn area from September 17th to 22nd, 2022, depositing 3.4 cm of rain (National Oceanic and Atmospheric Administration. NOAA NCEI. 2022). Due to logistics, road closures through Foresthill Road to access the Middle Fork, and hydraulic travel times (time for runoff to travel from burned area to sample locations), Teledyne ISCO 6712 autosamplers were placed on September 23rd, 2022 on both the North and Middle Forks of the American River, likely capturing the declining hydrograph, based on the DOM in the samples (there is no stream gage present on these forks of the River). Both samplers were started at 3pm on September 23rd and collected twenty-four 900 mL composite samples of storm runoff (300 mL every hour) over the course of 72 h. Samples were retrieved on September 27th, and placed on ice for transport to the laboratory for analysis.

2.2. Analytical methods

2.2.1. Sample preparation and water quality analyses

Samples were filtered through 0.7 μ m GF/F filters (pre-baked at 500 °C for 3 h) and stored at 4 °C. Dissolved organic carbon (DOC) and total dissolved nitrogen (TDN) were quantified with a Shimadzu TOC-L (Shimadzu Corp., Japan). Anions were analyzed with Thermo-Scientific Dionex ICS-6000 Ion Chromatograph (Dionex, Sunnyvale, CA, USA). Ammonium was analyzed with Hach Test Kits which conform to USEPA Method 350.1 (Hach, Loveland, CO, USA). In selected samples, metals were analyzed with inductively coupled plasma mass spectrometry (Shimadzu 2030, Shimadzu Corp., Japan). Dissolved organic nitrogen was calculated as the difference between TDN and dissolved inorganic nitrogen (DIN, the sum of ammonia (NH $_{+}^{+}$ -N), nitrate (NO $_{3}^{-}$ -N), and nitrite (NO $_{2}^{-}$ -N) concentrations). Calculations of DON in samples with

inorganic nitrogen concentrations greater than 60% of TDN are considered to have a substantial amount of propagated error and were discarded (Lee and Westerhoff, 2005).

UV absorbance from 190 to 1100 nm was analyzed with a Hach DR. 6000 UV-Vis spectrophotometer (Hach, Loveland, CO, USA) with a 1 cm quartz cuvette. E2/E3 ratio was calculated as the absorbance at 250 nm wavelength (E2) divided by the absorbance at 365 nm wavelength (E3) and is inversely correlated with the molecular weight of DOM (Peuravuori and Pihlaja, 1997). Fluorescence was measured using a Shimadzu RF-6000 Spectrofluorophotometer with a 1 cm quartz cuvette and LabSolutions RF v 1.17 software (Shimadzu, Japan). For Trout Creek samples, fluorescence was measured in samples with the highest and lowest DOC concentrations for each storm event and in samples for the subsequent month. For the Middle and North Forks of the American River, fluorescence was measured on the first, twelfth, and twenty-fourth samples, corresponding to the beginning, middle, and end of the sampling period. Excitation and emission slits were set to 5 nm. Excitation was conducted from 220 to 450 nm at 2 nm intervals, emission was measured from 220 to 550 nm at 0.5 nm intervals. Inner filter correction, Raman normalization, and blank subtraction were performed using the drEEM toolbox in Matlab (K. R. Murphy et al., 2013). The fluorescence index (FI) of samples was calculated as the ratio of emission intensities at 470 nm and 520 nm at the excitation wavelength of 370 nm (Jaffé et al., 2008; McKnight et al., 2001). High iron concentrations are known to interfere with the measurement of fluorescence indices and UV-Vis adsorption, however, interference is expected to be negligible because all but one sample had <0.03 mg Fe/L, measured by ICP-MS (McKnight et al., 2001; Poulin et al., 2014; Weishaar et al., 2003).

2.2.2. Chlorination and DBP analysis

The potential to form DBPs in untreated water samples was evaluated following Uniform Formation Conditions (UFC) as described by Summers et al. (1996). Though these treatment conditions do not perfectly represent conventionally treated drinking water, the experiments were designed to investigate overall changes to organic matter reactivity, rather than only that which passes conventional treatment, which varies from plant to plant and is thus hard to universally represent. Samples were buffered with 1 M borate solution (pH 8 ± 0.2) and chlorinated with 1 M borate-buffered sodium hypochlorite solutions (pH 8 \pm 0.2) at 20 ±1 °C. While borate may complex phenolic groups in humic substances (Schmitt-Kopplin et al., 1998), we preferred to use this buffer for comparability to other studies which follow the UFCs as described by Summers et al. Preliminary chlorine demand studies were performed with a series of three Cl₂:DOC ratios (1.2:1, 1.8:1, and 2.5:1), followed by incubation at room temperature for 24±1 hr. A chlorine dose was then selected which yielded a 1 \pm 0.4 mg/L Cl_2 residual after 24 hr and a 70 mL sample was then dosed accordingly. 10 mL of sample was removed to measure Cl2 residual after 24 hr to confirm a residual of 1 ± 0.4 mg/L Cl₂. Residual chlorine was quenched using 50 μ M ascorbic acid and 150 µL of 12 N hydrochloric acid, and the remaining 60 mL of the sample was stored for DBP analysis.

Quantification was conducted for four THMs (chloroform, bromodichloromethane (BDCM), dibromochloromethane (DBCM), and bromoform), nine HAAs (chloroacetic acid (CAA), dichloroacetic acid (DCAA), bromoacetic acid (BCAA), trichloroacetic acid (TCAA), bromochloroacetic acid (BCAA), bromodichloroacetic acid (BDCAA), dibromoacetic acid (DBAA), chlorodibromoacetic acid (CDBAA), and tribromoacetic acid (TBAA)), six HANs (bromochloroacetonitrile (BCAN), dibromoacetonitrile (DBAN), dichloroacetonitrile (DCAN), trichloroacetonitrile (TCAN), bromoacetonitrile (BAN), and chloroacetonitrile (CAN), and six HAMs (bromoacetamide (BAM), chloroacetamide (CAM), dichloroacetamide (DCAM), trichloroacetamide (TCAM), dibromoacetamide (DBAM), and bromochloroacetamide (BCAM)). Quantification was conducted using modified EPA 551.1 (THMs, HANs, and HAMs) and 552.2 (HAAs) (USEPA, 1995a, 1995b)

methods with gas chromatography electron capture detection (GC-ECD, Agilent 8860, Santa Clara, CA, USA) (Stewart et al., review). Bromine incorporation factor (BIF) was calculated to evaluate the potential to form more brominated DBPs based on equations found in Shukairy et al. (1994)

2.3. Statistical analysis

To assess relationships and temporal differences in water quality and DBP formation between samples, non-parametric tests were used to compare samples from different storm events, watersheds, and seasons [winter (December-February), spring (March-June), and Summer (June-September)] for the Caldor Fire. Non-parametric tests were used due to the seasonality and non-normality associated with environmental water quality data (Rong, 2011). For the Mosquito Fire, measured water quality characteristics were compared between burned and unburned watersheds using parametric t-tests. Pearson's correlation coefficient (r) was used to assess correlation. All statistical analyses were performed using GraphPad Prism version 9.4.1 for MacOS (GraphPad Software, San Diego, California, USA).

3. Results and discussion

To evaluate changes to water quality and reactivity to form DBPs in forested watersheds, we first focused on the initial flushes in Trout and Cold Creeks in the Caldor Fire study area and the North and South Forks of the American River in the Mosquito Fire study area. To evaluate long-term impacts, Trout Creek in the Caldor Fire watershed was sampled for 11 months following the wildfire occurrence.

3.1. Initial flushing events

3.1.1. DOC and DON

The Caldor Fire started in August 2021 and was fully contained on October 21, 2021. On October 17th, a total of 8.9 cm of snow fell as measured at the South Lake Tahoe Airport, 2.2 km from the study site. On October 22-23rd, 1.9 cm of rain fell with no snow accumulation. On October 25th, a storm starting as snow and changing to rain occurred, causing the largest peak flow since 2019 and three times greater than peak spring runoff in 2021. Samples taken during and immediately after this precipitation event had a strong odor of charred wood, though no visible pieces of wood or detritus were present in the samples. In Cold Creek (unburned by the Caldor Fire), DOC levels captured on October 5-7th had an average concentration of 2.5 mg C/L. In Trout Creek (burned by the Caldor Fire), DOC steadily increased from a low of 1.2 mg C/L on October 17 to a peak of 23.9 mg C/L on October 25, a 20x increase over one week (Fig. 2). DON in Trout Creek also reached its peak on October 25 (0.69 mg N/L), which is 17x greater than the average DON concentration recorded in Cold Creek (0.038 mg N/L). Both DOC and DON did not decrease to concentrations similar to pre-storm by 10:00 am, October 25th, the end of the high frequency, targeted, sampling event.

The Mosquito Fire started in September 2022 and was fully contained on October 22nd, 2022. In the Middle Fork of the American River (burned by the Mosquito Fire), DOC and DON concentrations steadily decreased over the course of 72 h of sampling that occurred during the first flushing event post-fire. This is reflective of the tail of the spike in mobilized organic matter being captured by the sampling event due to logistics in reaching the burn zone to capture the rising tail: road closures due to the active Mosquito Fire and unsafe travel on dirt roads due to rain. Neither sampling event was able to capture the rising tail of the precipitation-induced spikes due to these logistical issues or soil subsidence causing the Trout Creek sampler to overturn, which caused the loss of the first 14 samples and reduced volume of the remaining samples. Concentrations in the unburned fork exhibited no trend of DOC or DON (i.e., roughly the same over the sampling period) due to a lack of

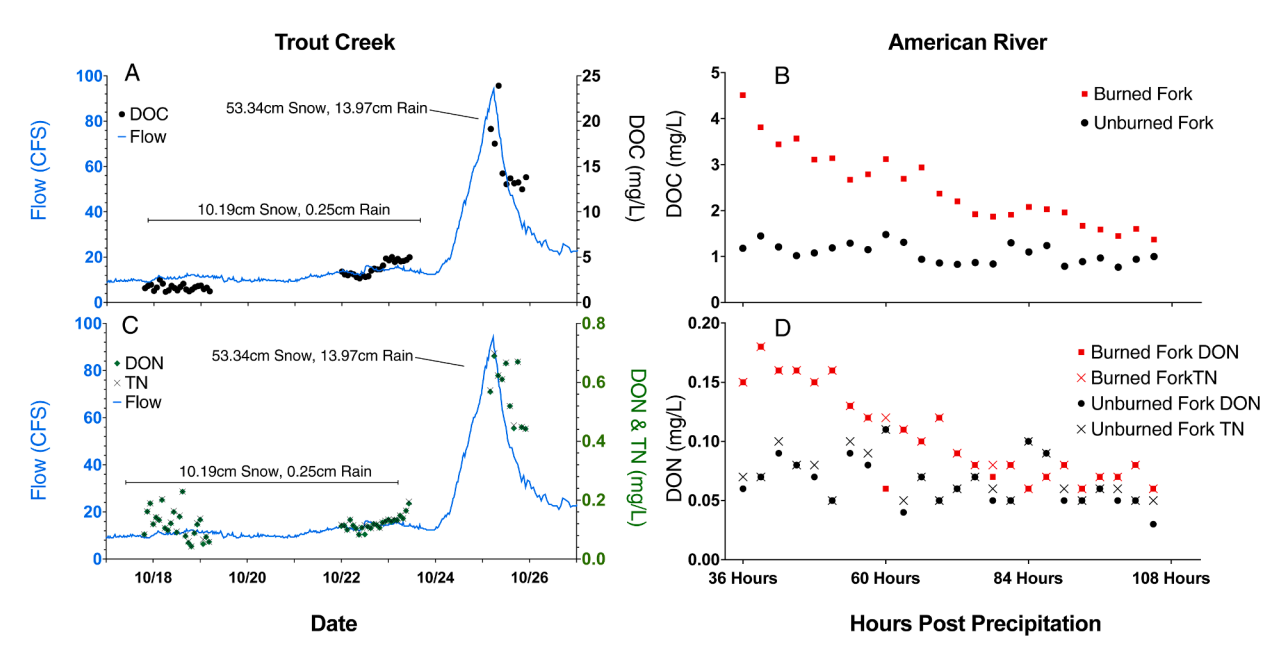


Fig. 2. Trout Creek (burned fork only) and American River (burned and unburned) DOC, DON, and TN concentrations. Runoff from three storm events was captured in Trout Creek (affected by the Caldor Fire), while runoff from one storm was captured concurrently in the burned and unburned forks of the American River. The American River does not have a corresponding hydrograph because there is no gaging station on either fork. In the American River, the last precipitation occurred Sept. 22 while peak precipitation occurred Sept. 20. Autosamplers in the American River were started at 3:00pm Sept. 23.

mobilized organic matter. The relatively quick decrease in DOC and DON in the American River suggests that water quality in burned catchments may return to levels comparable to unburned watersheds as little as a few days of storms. This was not well reflected in the Trout Creek dataset due to the sampling timespan being intended to capture the initial rise, peak, and fall of storm runoff.

3.1.2. Disinfection byproduct precursors, yield, and speciation

In Trout Creek, the greatest formation of THMs, HAAs, and N-DBPs (total of HAN and HAM) during the October 25th flush were 613 μ g/L, 1301 μ g/L, and 128 μ g/L, respectively (Fig. 3). Total DBP formation in the burned watershed was 13x greater than in the paired, unburned watershed, (samples taken Oct. 5 – 7th, Fig. 3, panel A), which had maxima of 80 μ g/L, 70 μ g/L, and 5 μ g/L of TTHMs, HAAs, and N-DBPs, respectively. Similarly, in the American River, the burned fork exhibited higher formation of TTHMs, HAAs, HANs, and HAMs in the burned vs the unburned forks; 44.8 μ g/L, 37.5 μ g/L, 6.7 μ g/L, and 6.9 μ g/L greater in the burned compared to the unburned fork (Fig. 4).

DBP speciation was also altered by storm events between burned and unburned watersheds in the Caldor Fire area, indicating changes to DOM characteristics. For example, in the Trout Creek watershed prior to the October 22nd storm, DBP speciation was similar in the paired burned and unburned creeks (Fig. 3, panels A, C, and E). Over the course of the storm, however, HAA and HAN became the dominant C- and N-DBP species, over TTHM and HAM, which dominated pre-storm. These changes in DBP speciation have not been noted in similar watershed-scale studies (Hohner et al., 2016; Uzun et al., 2020; Writer et al., 2014). However, this was not reflected in the Mosquito Fire study area. Only one storm event was captured and there was no substantial change in DBP speciation in either fork over the sampling period, suggesting somewhat different changes to DOM composition caused by the two fires

A shift in the DBP reactivity of the organic matter was observable. In Trout Creek, HAA yields reached their maxima for the year (see Longterm Effects for further discussion) during the October 22nd storm and remained elevated through the October 25th storm (Fig. 3, panels B, D, and F). HAA yields from these two storm events were higher than those of the October 18th storm and the unburned watershed (53.37 vs 35.00

& 16.82 µg HAA UFC/mg DOC, respectively, p < 0.05). TTHM yields declined over the course of the successive October 22nd and October 25th storms and reached their lowest during the October 25th storm. TTHM yields during the October 25th storm were shown to be significantly lower than the October 17th and 22nd storms (median yields of 30.78 and 41.35 μ g THM UFC/mg DOC respectively, p < 0.05). The shift in HAA and TTHM yields may potentially be explained by the higher DON concentrations measured during those storm events, as high DON concentrations have been shown to drive a shift to HAA formation over THM (Westerhoff and Mash, 2002). DOC normalized HAN yields on October 25th were not significantly different from the previous two storms. All three storms captured in Trout Creek did contain higher HAN yields compared to the unburned reference watershed, however (p < 0.05). HAM yields were higher on October 25th than the control creek and the previous two storms. However, in the American River, C-DBP yields were not found to be significantly different between burned vs unburned forks (p < 0.05), but HAN and HAM yields were higher (p < 0.05) 0.05) in the burned fork (Fig. 4). Together, the data from two fires suggest that DBP precursor material is altered to varying degrees and these changes are specific to the fire. This, along with work showing greater HAA5 and HAN4 yields in fire-affected watersheds, shows that increased HAA and HAN yields may also be a general trend following wildfire (Hohner et al., 2016; Writer et al., 2014).

The October 25th storm in Trout Creek caused the greatest TTHM, HAN, and HAM BIFs when compared to the unburned watershed and previous storm storms (p < 0.05). The burned fork of the American River also had 0.67 µg/L greater (p < 0.05) formation of brominated species on average, compared to the unburned fork. TTHM BIF values were greater in the burned fork of the American River, while HAA BIF was greater in the unburned fork (p < 0.05). HAN and HAM BIF values were not significantly different between burned and unburned forks (p > 0.05). This indicates that substantial early flushing events in burned watersheds cause greater bromine incorporation and formation of brominated DBPs. Higher BIF values in burned watersheds compared to unburned reference watersheds have previously been observed by Uzun et al. (2020). Brominated species are generally more toxic than chlorinated analogs (Hanigan et al., 2017; Wagner and Plewa, 2017) and therefore storm runoff from burned areas may create more toxic

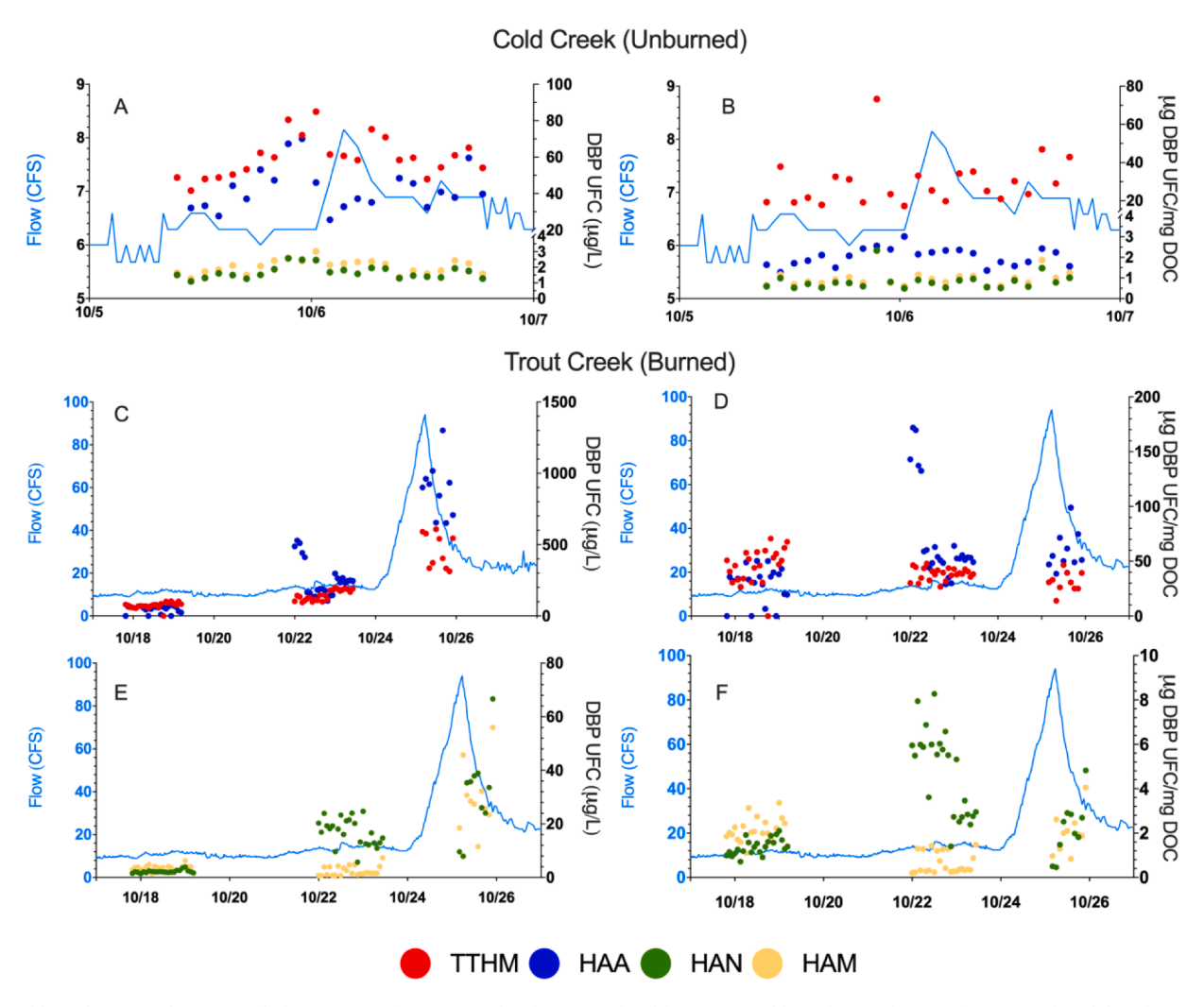


Fig. 3. Cold Creek (top) and Trout Creek (bottom) DBP formation and carbon normalized formation. Cold Creek is a tributary of Trout Creek and thus the same USGS gaging station data downstream of the confluence was used to produce the hydrograph.

mixtures of DBPs compared to unburned areas.

3.1.3. NOM optical characteristics

In Trout Creek, the FI of samples taken during the first two storms post-fire ranged from 1.59 to 1.84, and 1.25 on October 25th. The FI of the two samples measured in the unburned creek were 1.65 and 1.61. Fluorescence data of the October 25th corresponding with peak runoff was omitted as the sum of absorbance at the excitation and emission wavelengths was above 1.5, which leads to inaccuracies in inner filter correction, and no sample remained to reanalyze at 2x dilution (Kothawala et al., 2013). The burned fork of the American River exhibited higher FI (1.71-1.77) compared to the unburned fork (1.59–1.67), indicating more microbially derived DOM (McKnight et al., 2001). Both Hohner et al. (2016) and Uzun et al. (2020) have noted higher FI values in burned watersheds compared to unburned, reference watersheds. FI has also been used as a measure of changes in the composition and molecular size of DOM, high higher FI values indicating less complexity and smaller molecular size (Cawley et al., 2017; Podgorski et al., 2012; Romera-Castillo et al., 2014; Wang et al., 2015). This indicates that fire may initially result in the flushing of smaller molecular organic matter.

Regarding aromaticity of the organic matter present, in Trout Creek, the storm on October 25th had the lowest average SUVA₂₅₄ values of the year compared to the two prior storms on October 17th and 22nd, and the following winter, spring, and summer (p < 0.05). The unburned

creek of the Caldor Fire exhibited lower SUVA $_{254}$ than the two storms on October 17th and 22nd and October 25th (p < 0.05). Paired t-tests indicated that SUVA $_{254}$ in the burned fork of the American River was significantly higher (p < 0.05) compared to the unburned fork. Taken together, these results indicate that fire does indeed increase the aromaticity of DOM, but the degree to which differs between storm events. Although others have demonstrated a relationship between SUVA and aromaticity in pyrogenic DOM, it should be noted that this is a surrogate and should not be confused as a direct measure of aromaticity (Chen et al., 2022; Yan et al., 2022).

In both forks of the American River, along with the unburned creek from the Caldor Fire burn area, $SUVA_{254}$ was negatively but nonsignificantly (p>0.05) correlated with TTHM, HAA, HAM, and HAN. This contrasts with earlier works showing that THM and HAA formation has a positive correlation with $SUVA_{254}$ (Hua et al., 2015). It has been shown that $SUVA_{254}$ values from leachate of ash are highest for white ash (high burn severity), followed by unburned material, then black ash (moderate burn severity) (Wang et al., 2016). Given the lower SUVA values of moderate burn severity soil, this could indicate that moderately burned material was being washed into the burned watersheds during the storm, as much of both (Middle fork of American River and Trout Creek) upstream areas was of low-medium burn severity.

3.1.4. Nutrients

In Trout Creek, NO_3^- was generally below the detection limit (0.004

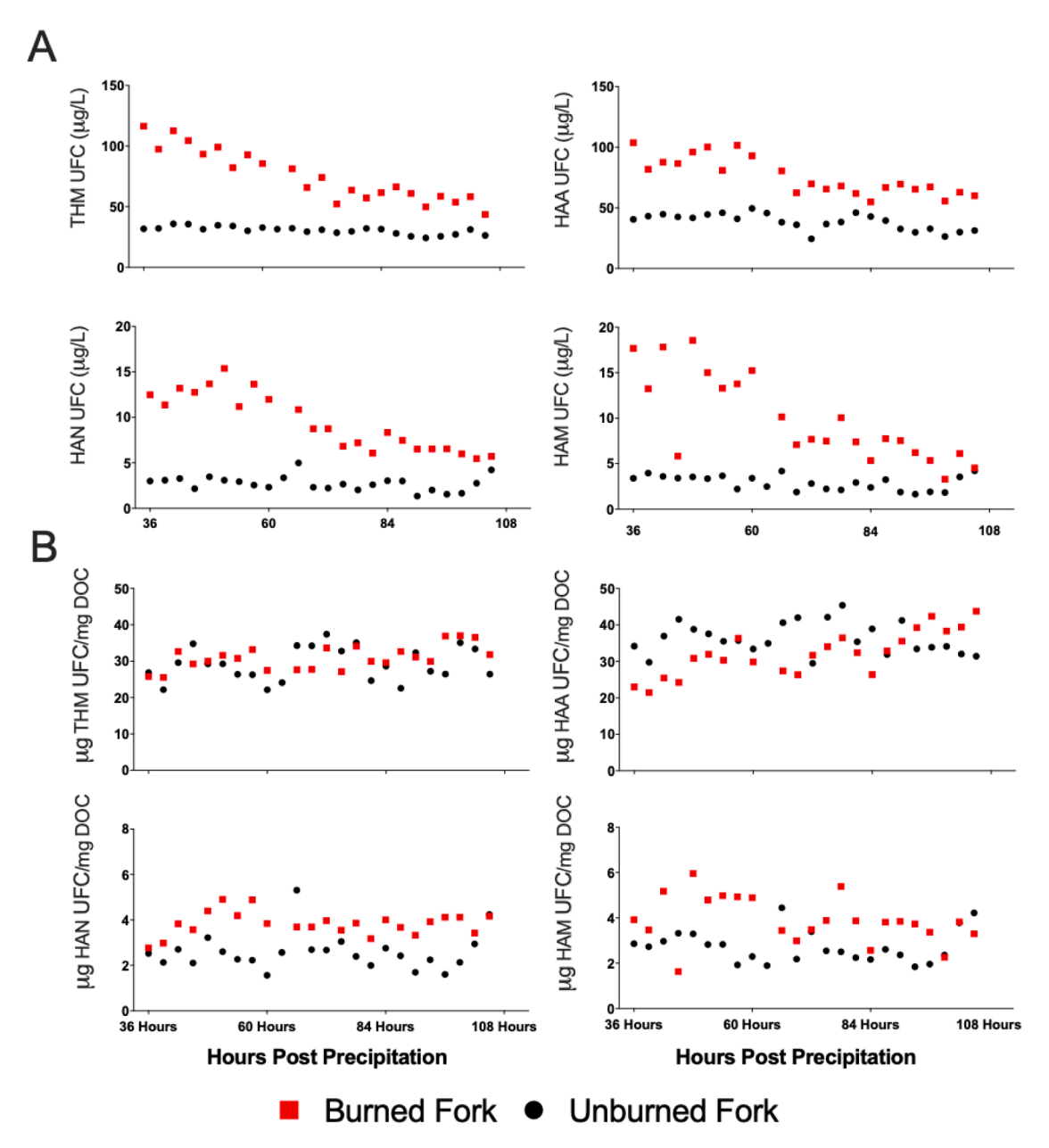


Fig. 4. Total (A) and DOC normalized (B) TTHM, HAA, HAN, and HAM formation in the North and Middle Forks of the American River. The American River does not have a corresponding hydrograph because there is no gaging station on either fork. The last precipitation occurred Sept. 22 while peak precipitation occurred Sept. 20. Autosamplers in the American River were started at 3:00pm Sept. 23.

mg NO_3^--N/L) through the October 18th storm, except on two occasions (0.005 and 0.045 mg NO_3^--N/L , respectively). Starting October 22nd and extending through October 25th NO_3^- was detectable with average concentrations of 0.003 mg NO_3^--N/L . In the burned fork of the American River, NO_3^- was detected on one occasion, but was similar to the unburned fork. The absence of inorganic nitrogen in samples from the burned watershed may be explained by the time elapsed between the wildfire and storm occurrences. After the fire, biotic and abiotic processes transform organic N into more bioavailable forms which then become bound in organic matter or lost via denitrification (Knicker, 2007). It is possible that NO_3^- present in the burned watershed was mobilized sooner than the sampling period but was continuously generated in the unburned area due to continuous nitrification of reduced nitrogen by biological nitrification.

Also in Trout Creek, phosphate concentrations increased over the course of the October 2021 storms, ranging from 0.05 mg P/L on October 17th to its highest concentration, 0.31 mg P/L, on October 25th.

In the American River, the burned fork had higher phosphate concentrations than the unburned fork, though the difference was not statistically different (paired *t*-test). The impact of wildfire on nutrients in the short term may differ between watersheds, but large spikes in phosphate concentrations are possible after wildfire.

3.1.5. Predictability of adverse drinking water intake quality

Linear regression of water quality parameters as predictors of TTHM, HAA, HAN, and HAM during initial flushes was conducted with the intent to demonstrate that water utilities may be able to predict sharp increases in treated water DBP formation based on these relatively simple metrics (SI, Eqs. 1–8). In brief, our findings agree well with findings from others developed in unburned watersheds (Chen and Westerhoff, 2010; Chowdhury et al., 2009). DOC/DON ratios were strong predictors of TTHM and HAN. In the burned fork of the American River, the best predictor of TTHM, HAA, HAN, and HAM was DOC (R^2 = 0.91, 0.71, 0.74, 0.61, respectively, p < 0.05). Regression models may be

useful for utilities to build with their post-wildfire data to predict future impacts in source watersheds.

3.2. Long-term effects

3.2.1. DOC and DON

Only the Caldor Fire study site was investigated for long-term effects due to the logistical challenges of long-term maintenance of samplers across the Sierra Nevada Mountains in the American River watershed. After the storms in October, DOC declined through February, but then rose again and peaked in early April (4.9 mg C/L), corresponding with a localized maximum in spring runoff flow rate (Fig. SI-3). DOC concentrations stabilized in May at 2.6 \pm 0.6 mg C/L, until the end of the sampling campaign in September, despite peak runoff occurring in late May. DOC has been shown by others to increase in spring runoff from both burned and unburned watersheds, though DOC concentrations in moderately burned watersheds are known to remain elevated up to 14 years after wildfire (Hornberger et al., 1994; Murphy et al., 2015; Rhoades et al., 2019). Compared to samples taken from the unburned adjacent creek in April-September, the burned creek had an average 0.97 mg/L higher DOC concentration (n = 11, p < 0.05), agreeing that DOC concentrations are increased over the long-term post-wildfire.

In late March, total nitrogen (TN) reached a maximum for the long-term sampling period, again corresponding to spring snowmelt and runoff, although the maximum concentration was lower than the October 25th flush (0.69 vs 0.38 mg N/L). DON concentrations steadily decreased from 0.13 mg DON/L over the course of April and May, stabilizing in June (0.07 \pm 0.02 mg N/L) (Fig. SI-3). Compared to paired samples in the unburned creek, average TN and DON concentrations in the burned creek were 0.04 mg N/L and 0.03 mg DON/L higher, respectively (p < 0.05). This indicates that modest long-term increases in TN and DON occurred post-wildfire.

3.2.2. Disinfection byproduct formation and yield

Approximately 4 months after the fire was extinguished (late December), the potential to form C-DBPs increased rapidly coinciding with a large precipitation event, although this event did not cause substantial differences in HAN and HAM precursor loadings (Fig. 5). As spring runoff began and progressed, DBP concentrations of all species begin to increase. C-DBP concentrations peaked in early April before a gradual decline as the stream returned to summer baseflow conditions, although these peaks in the potential to form C-DBPs do not perfectly coincide with peak runoff, occurring somewhat earlier. Greater DON concentrations resulted in increased HAM and HAN formation (Pearson r=0.64 and 0.6, p<0.05, respectively). For most of the post-fire sampling period, December 2021 to September 2022, HAA formation was most strongly and significantly correlated with DON. These findings agree with others that have demonstrated that DON is associated with

increased N-DBP and HAA formation, and moderate burning increases DON concentrations in soil organic matter (Knicker et al., 2005).

C- and N-DBP yields began increasing in the spring, also coinciding with spring runoff. Increased C-DBP yields during spring runoff from fire-affected watersheds have also been noted by Writer et al. (2014) and Hohner et al. (2016), though both authors stated it is hard to separate the effect of fire from other confounding factors. To separate confounding factors such as seasonal NOM flushing, a limited paired analysis was conducted with samples from the unburned creek (n = 11). HAN yields were greater in the burned creek (p < 0.05) but not significantly different for other species, suggesting that DOM had returned to baseline characteristics. HAA, HAN, and HAM yields continued to increase throughout the summer when the highest median yields of both HAN and HAM occurred. This is indicative of the temporal variability in C and N-DBP precursor reactivity, similar to findings by Hohner et al. (2016) and Wang et al. (2016). The E2/E3 ratio was a significant predictor for both TTHM and HAM formation (SI, Eqs. 9-12). The largest E2/E3 ratios were found in mid-late March, followed by the October 25 storm. The link between E2/E3 ratios and TTHM, and HAM concentration indicates that smaller molecular size DOM is a driver of their formation. Though we were unable to measure molecular size distribution in our samples directly, Hohner et al. (2019) were able to demonstrate that heating soil decreased molecular weight as measured via SEC-UVA and that these heated soil samples also displayed higher E2:E3 ratios. Further, the study demonstrated this in soil from two separate locations in Colorado and one location in New York. DOC normalized formation of N-DBPs was weakly negative and not significantly correlated with DON. Post-fire, the net increase of mobilized C and N caused an increase in N-DBP and HAA formation, although the pyrogenic carbon was generally less reactive in forming N-DBPs, suggesting treatment strategies intended to remove C for DBP control may also effectively mitigate DBPs formed from greater concentrations of pyrogenic carbon, which is less reactive.

3.2.3. NOM characteristics

Over the longer term, SUVA $_{254}$ and FI values did not change significantly, and remained within the range of 4.21 ± 0.88 and 1.61 ± 0.04 , respectively, comparable to values from the unburned paired watershed in October 2021. SUVA $_{254}$ was higher but not significantly different from paired values in the unburned watershed (0.15, p=0.68). Together, these suggest a relatively rapid transition in optical properties to a steady state post-fire and the limited potential of these properties to serve as surrogates for wildfire effects over the longer term.

3.2.4. Nutrients

NH₄⁺-N concentrations were generally below detection limit throughout the sampling campaign but were maximized in early March 2022 (0.016 mg NH₄⁺-N/L). NO₃⁻-N peaked in late March (0.43 mg NO₃⁻-

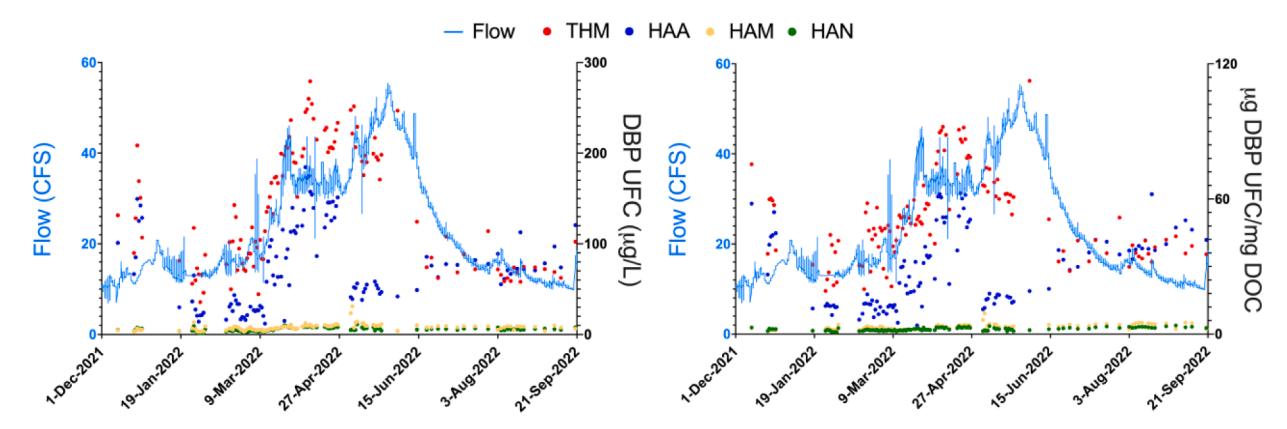


Fig. 5. Total and DOC normalized THM, HAA, HAN, and HAMs in Trout Creek.

N/L) and declined to concentrations below the detection limit (0.015 mg N/L) in April, before a short spike in mid-August (0.18 mg NO $_3$ -N/L) when the concentration began to increase again. Mean NO $_3$ -N/L concentrations were higher but not significantly different from paired values in the unburned watershed (p > 0.05). The mean concentration of samples from October 2021 to September 2022 was 0.09 mg NO $_3$ -N/L.

The average TP concentration of the Trout Creek samples from October 17, 2021, through September 20, 2022, is 0.09 mg P/L. Compared to paired values in the unburned reference watershed, TP concentrations in the burned watershed were 0.028 ± 0.012 mg P/L higher (p > 0.05). The average contribution of phosphate to TP concentrations was $73\pm35\%$ of TP. TP concentrations remained above the average through May. Elevated nutrients increase eutrophication risk, which may increase DBP concentrations and threaten source water quality (Bladon et al., 2014; Tsai et al., 2019).

4. Conclusions and implications for water utilities

In the short term after wildfire, severe impairments in water quality can occur during storm events. DOC concentrations during flushing events in the American River and Trout Creek increased to as much as 4.8x (4.9 to 23.9 mg C/L) the concentrations of the paired, unburned watersheds, and remained elevated for up to 4 days post-storm. Wildfire may also cause moderate increases in both DOC and DON concentrations compared to unburned watersheds within the first year. Increased DOC resulted in as much as a 13x increase in total DBP formation (all DBPs measured, or 7x and 26x for the regulated THMs and HAAs, respectively). DBP formation generally diminished by half over the course of a few hours but remained elevated for several days after peak precipitation. Comparatively, DBP formation fell back to base conditions within 36 h in unburned watersheds. This shows that although the largest spikes in DBP concentrations occur over a relatively short period, they may stay elevated for longer periods (several days) compared to a previous unburned state. DOM in storm runoff also had different reactivity in some cases, leading to the formation of more toxic DBPs, such as HAM, HAN, and brominated species. These changes in DOM reactivity occurred only in storm runoff, indicating that wildfire does not permanently alter DBP precursors in burned watersheds.

The relatively short nature of the most severe degradation in water quality presents an opportunity for drinking water treatment plants to plan for precipitation events immediately following fire and potentially briefly shut down affected intakes during these events, relying on banked water in the distribution system. However, given that DOC remained elevated for several days following precipitation, drinking water treatment plants may face elevated DBP concentrations after flushing events for a period that may exceed their ability to rely on treated and banked water. This may pose a substantial threat to drinking water treatment facilities as wildfires increase in frequency. Further, initial flushes of storm runoff had higher concentrations of DON, but inorganic nitrogen did not increase until months post-wildfire. This may also impact a drinking water treatment plant's ability to meet primary drinking water standards for nitrate. Elevated levels of nitrogen and phosphate in both the short and long term may exacerbate eutrophication issues in impoundments, which may lead to algal blooms that can increase treatment challenges (Emelko et al., 2011; Smith et al., 2011; Tsai et al., 2019). Based on limited evidence published by others, these effects may be partially or wholly mitigated by operational changes to the treatment plant (e.g., increased coagulant dose, increased filter backwash frequency), but these operational changes have only been studied in a limited number of experiments/publications, highlighting an urgent need for additional research (Chen et al., 2020; Hohner, 2016; Writer et al., 2014).

Declaration of Competing Interest

The authors declare that they have no known competing financial

interests or personal relationships that could have appeared to influence the work reported in this paper.

Data availability

The raw data is contained in the SI.

Acknowledgments

We gratefully acknowledge support for this research from the National Science Foundation (OIA – 2229313) and the US Department of Education Graduate Assistance in Areas of National Need Program. We gratefully acknowledge the initial sampling conducted at the Caldor Fire by Nicholas Yensen and the assistance of Kevin Stewart, Jackson Marsten, and Karla Henricksen in sampler placement. The authors wish to thank the staff of the Auburn State Recreation Area for their assistance.

Supplementary materials

Supplementary material associated with this article can be found, in the online version, at doi:10.1016/j.watres.2023.120474.

References

- Abatzoglou, J.T., Williams, A.P., 2016. Impact of anthropogenic climate change on wildfire across western US forests. Proc. Natl. Acad. Sci. U. S. A. 113 (42), 11770–11775. https://doi.org/10.1073/pnas.1607171113.
- Allen-Diaz, B., Hammerling, E., Campbell, C., 1998. Comparison of standard water quality sampling with simpler procedures. J. Soil Water Conserv. 53 (1), 42. LP–45. http://www.jswconline.org/content/53/1/42.abstract.
- Beyers, Jan L., Brown, James K., Busse, Matt D., DeBano, Leonard F., Elliot, William J., Ffolliott, Peter F., Jacoby, Gerald R., Knoepp, Jennifer D., Landsberg, Johanna D., Neary, Daniel G., Reardon, James R., Rinne, John N., Robichaud, Peter R., Ryan, Kevin C., Arthur, M.J.Z., 2005. Effects of fire on soil and water. Catena 9 (2), 1–5. https://doi.org/10.1016/j.catena.2008.03.011.
- Bladon, K.D., Emelko, M.B., Silins, U., Stone, M., 2014. Wildfire and the future of water supply. Environ. Sci. Technol. 48, 8936–8943.
- Bond, T., Huang, J., Templeton, M.R., Graham, N., 2011. Occurrence and control of nitrogenous disinfection by-products in drinking water—a review. Water Res. 45 (15), 4341–4354. https://doi.org/10.1016/j.watres.2011.05.034.
- Cawley, K.M., Hohner, A.K., Podgorski, D.C., Cooper, W.T., Korak, J.A., Rosario-Ortiz, F. L., 2017. Molecular and spectroscopic characterization of water-extractable organic matter from thermally altered soils reveal insight into disinfection byproduct precursors. Environ. Sci. Technol. 51 (2), 771–779. https://doi.org/10.1021/acs.est.6b05126.
- Certini, G., 2005. Effects of fire on properties of forest soils: a review. Oecologia 143 (1), 1–10. https://doi.org/10.1007/s00442-004-1788-8.
- Chen, B., Westerhoff, P., 2010. Predicting disinfection by-product formation potential in water. Water Res. 44 (13), 3755–3762. https://doi.org/10.1016/j. watres.2010.04.009.
- Chen, H., Ersan, M.S., Tolić, N., Chu, R.K., Karanfil, T., Chow, A.T., 2022. Chemical characterization of dissolved organic matter as disinfection byproduct precursors by UV/fluorescence and ESI FT-ICR MS after smoldering combustion of leaf needles and woody trunks of pine (Pinus jeffreyi). Water Res. 209 (December 2021) https://doi.org/10.1016/j.watres.2021.117962.
- Chen, H., Uzun, H., Chow, A.T., Karanfil, T., 2020. Low water treatability efficiency of wildfire-induced dissolved organic matter and disinfection by-product precursors. Water Res. 184 https://doi.org/10.1016/j.watres.2020.116111.
- Chowdhury, S., Champagne, P., McLellan, P.J., 2009. Models for predicting disinfection byproduct (DBP) formation in drinking waters: a chronological review. Sci. Total Environ. 407 (14), 4189–4206. https://doi.org/10.1016/j.scitotenv.2009.04.006.
- Dahlgren, R.A., Boettinger, J.L., Huntington, G.L., Amundson, R.G., 1997. Soil development along an elevational transect in the western Sierra Nevada, California. Geoderma 78 (3–4), 207–236. https://doi.org/10.1016/S0016-7061(97)00034-7.
- Dennison, Philip E., Brewer, Simon C., Arnold, James D., 2014. Large wildfire trends in the western United States, 1984–2011. Geophys. Res. Lett. 41, 2928–2933. https://doi.org/10.1002/2014GL059576.
- Doerr, S.H., Shakesby, R.A., Walsh, R.P.D., 2000. Soil water repellency: its causes, characteristics and hydro-geomorphological significance. Earth Sci. Rev. 51 (1–4), 33–65. https://doi.org/10.1016/S0012-8252(00)00011-8.
- Ellsworth, T., Stamer, M., 2021. 2021 Caldor Fire Burned Area Emergency Response. htt ps://inciweb.nwcg.gov/photos/CAENF/2021-09-12-2027-Caldor-PostFire-BAER/ related_files/pict20210921-101423-0.pdf.
- Emelko, M.B., Silins, U., Bladon, K.D., Stone, M., 2011. Implications of land disturbance on drinking water treatability in a changing climate: demonstrating the need for "

- source water supply and protection" strategies. Water Res. 45 (2), 461–472. https://doi.org/10.1016/j.watres.2010.08.051.
- Fernández, I., Cabaneiro, A., Carballas, T., 1997. Organic matter changes immediately after a wildfire in an atlantic forest soil and comparison with laboratory soil heating. Soil Biol. Biochem. 29 (1), 1–11. https://doi.org/10.1016/S0038-0717(96)00289-1.
- Hanigan, D., Truong, L., Simonich, M., Tanguay, R., Westerhoff, P., 2017. Zebrafish embryo toxicity of 15 chlorinated, brominated, and iodinated disinfection byproducts. J. Environ. Sci. 58, 302–310. https://doi.org/10.1016/j.jes.2017.05.008.
- Hohner, A., 2016. Wildfire Disturbances To Water Quality: Implications for Drinking Water Treatment. Proquest Dissertations Publishing.
- Hohner, A.K., Cawley, K., Oropeza, J., Summers, R.S., Rosario-Ortiz, F.L., 2016. Drinking water treatment response following a Colorado wildfire. Water Res. 105, 187–198. https://doi.org/10.1016/j.watres.2016.08.034.
- Hohner, A.K., Rhoades, C.C., Wilkerson, P., Rosario-Ortiz, F.L., 2019a. Wildfires alter forest watersheds and threaten drinking water quality. Acc. Chem. Res. 52 (5), 1234–1244. https://doi.org/10.1021/acs.accounts.8b00670.
- Hohner, A.K., Rosario-Ortiz, F., Summers, S., 2019b. Laboratory Simulation of Postfire Effects On Conventional Drinking Water Treatment and Disinfection Byproduct Formation. https://doi.org/10.1002/aws2.1155. May, 1–17.
- Hornberger, G.M., Bencala, K.E., McKnight, D.M., 1994. Hydrological controls on dissolved organic carbon during snowmelt in the Snake River near Montezuma, Colorado. Biogeochemistry 25 (3), 147–165. https://doi.org/10.1007/BF00024390.
- Hua, G., Reckhow, D.A., Abusallout, I., 2015. Correlation between SUVA and DBP formation during chlorination and chloramination of NOM fractions from different sources. Chemosphere 130, 82–89. https://doi.org/10.1016/j.chemosphere.2015.03.039.
- Jaffé, R., McKnight, D., Maie, N., Cory, R., McDowell, W.H., Campbell, J.L., 2008. Spatial and temporal variations in DOM composition in ecosystems: the importance of longterm monitoring of optical properties. J. Geophys. Res. 113 (4), 1–15. https://doi. org/10.1029/2008.IG000683.
- Komaki, Y., Mariñas, B.J., Plewa, M.J., 2014. Toxicity of drinking water disinfection byproducts: cell cycle alterations induced by the monohaloacetonitriles. Environ. Sci. Technol. 48 (19), 11662–11669. https://doi.org/10.1021/es5032344.
- Korfmacher, J.L., Musselman, R.C., 2007. Evaluation of storage and filtration protocols for alpine/subalpine lake water quality samples. Environ. Monit. Assess. 131 (1–3), 107–116. https://doi.org/10.1007/s10661-006-9460-x.
- Kothawala, D.N., Murphy, K.R., Stedmon, C.A., Weyhenmeyer, G.A., Tranvik, L.J., 2013. Inner filter correction of dissolved organic matter fluorescence. Limnol. Oceanogr. 11 (DEC), 616–630. https://doi.org/10.4319/lom.2013.11.616.
- Knicker, H., 2007. How does fire affect the nature and stability of soil organic nitrogen and carbon? A review. Biogeochemistry 85 (1), 91–118. https://doi.org/10.1007/ s10533-007-9104-4.
- Knicker, H., González-Vila, F.J., Polvillo, O., González, J.A., Almendros, G., 2005. Fire-induced transformation of C- and N- forms in different organic soil fractions from a Dystric Cambisol under a Mediterranean pine forest (Pinus pinaster). Soil Biol. Biochem. 37 (4), 701–718. https://doi.org/10.1016/j.soilbio.2004.09.008.
- Krasner, S.W., Weinberg, H.S., Richardson, S.D., Pastor, S.J., Chinn, R., Sclimenti, M.J., Onstad, G.D., Thruston, A.D., 2006. Occurrence of a new generation of disinfection byproducts. Environ. Sci. Technol. 40 (23), 7175–7185. https://doi.org/10.1021/ cp/607821
- Le Roux, J., Nihemaiti, M., Croué, J.P., 2016. The role of aromatic precursors in the formation of haloacetamides by chloramination of dissolved organic matter. Water Res. 88, 371–379. https://doi.org/10.1016/j.watres.2015.10.036.
- Lee, W., Westerhoff, P., 2005. Dissolved Organic Nitrogen Measurement Using Dialysis Pretreatment. Environ. Sci. Technol. 39 (3), 879–884.
- Linge, K.L., Kristiana, I., Liew, D., Holman, A., Joll, C.A., 2020. Halogenated semivolatile acetonitriles as chloramination disinfection by-products in water treatment: a new formation pathway from activated aromatic compounds. Environ. Sci. 22 (3), 653–662. https://doi.org/10.1039/c9em00603f.
- Liu, N., Caldwell, P.V., Dobbs, G.R., Miniat, C.F., Bolstad, P.V., Nelson, S.A.C., Sun, G., 2021. Forested lands dominate drinking water supply in the conterminous United States. Environ. Res. Lett. 16 (8) https://doi.org/10.1088/1748-9326/ac09b0.
- McKay, G., Hohner, A.K., Rosario-Ortiz, F.L., 2020. Use of optical properties for evaluating the presence of pyrogenic organic matter in thermally altered soil leachates. Environ. Sci. 22 (4), 981–992. https://doi.org/10.1039/c9em00413k
- McKnight, D.M., Boyer, E.W., Westerhoff, P.K., Doran, P.T., Kulbe, T., Andersen, D.T., 2001. Spectrofluorometric characterization of dissolved organic matter for indication of precursor organic material and aromaticity. Limnol. Oceanogr. 46 (1), 38–48. https://doi.org/10.4319/lo.2001.46.1.0038.
- Mosquito Post-Fire BAER Assessment Report. 2022. https://inciweb.nwcg.gov/incident -publication/catnf-mosquito-postfire-baer/mosquito-postfire-baer-assessment-report -released
- Murphy, K.R., Stedmon, C.A., Graeber, D., Bro, R., 2013. Fluorescence spectroscopy and multi-way techniques. PARAFAC. Anal. Methods 5 (23), 6557–6566. https://doi. org/10.1039/c3ay41160e.
- Murphy, S.F., Writer, J.H., McCleskey, R.B., Martin, D.A., 2015. The role of precipitation type, intensity, and spatial distribution in source water quality after wildfire. Environ. Res. Lett. 10 (8) https://doi.org/10.1088/1748-9326/10/8/084007.
- National Oceanic and Atmospheric Administration, 1997. Heavy Precipitation Event December 26, 1996 - January 3. https://cnrfc.noaa.gov/storm_summaries/jan1997s
- National Oceanic and Atmospheric Administration. NOAA NCEI. (2022). https://www.ncei.noaa.gov.
- Peuravuori, J., Pihlaja, K., 1997. Molecular size distribution and spectroscopic properties of aquatic humic substances. Anal. Chim. Acta 337 (2), 133–149. https://doi.org/ 10.1016/S0003-2670(96)00412-6.

- Podgorski, D.C., Hamdan, R., McKenna, A.M., Nyadong, L., Rodgers, R.P., Marshall, A.G., Cooper, W.T., 2012. Characterization of pyrogenic black carbon by desorption atmospheric pressure photoionization fourier transform ion cyclotron resonance mass spectrometry. Anal. Chem. 84 (3), 1281–1287. https://doi.org/10.1021/ ac202166x.
- Poulin, B.A., Ryan, J.N., Aiken, G.R., 2014. Effects of iron on optical properties of dissolved organic matter. Environ. Sci. Technol. 48 (17), 10098–10106. https://doi. org/10.1021/es502670r
- Revchuk, A.D., Suffet, I.H., 2013. Effect of wildfires on physicochemical changes of watershed dissolved organic matter. Water Environ. Res. 86 (4), 372–381. https:// doi.org/10.2175/106143013x13736496909671.
- Rhoades, C.C., Chow, A.T., Covino, T.P., Fegel, T.S., Pierson, D.N., Rhea, A.E., 2019. The legacy of a severe wildfire on stream nitrogen and carbon in headwater catchments. Ecosystems 22 (3), 643–657. https://doi.org/10.1007/s10021-018-0293-6.
- Richardson, S.D., Plewa, M.J., Wagner, E.D., Schoeny, R., DeMarini, D.M., 2007. Occurrence, genotoxicity, and carcinogenicity of regulated and emerging disinfection by-products in drinking water: a review and roadmap for research. Mutat. Res. 636 (1–3), 178–242. https://doi.org/10.1016/j.mrrev.2007.09.001.
- Romera-Castillo, C., Chen, M., Yamashita, Y., Jaffé, R., 2014. Fluorescence characteristics of size-fractionated dissolved organic matter: implications for a molecular assembly based structure? Water Res. 55, 40–51. https://doi.org/10.1016/j.watres.2014.02.017.
- Rong, Y., 2011. Practical Environmental Statistics and Data Analysis. ILM Publications. Samson, C.C., Seidel, C.J., 2022. Assessing national HAA9 occurrence and impacts of a potential HAA9 regulation. AWWA Water Sci. 4 (6), 1–18. https://doi.org/10.1002/ aws2.1312.
- Sanchez, N.P., Skeriotis, A.T., Miller, C.M., 2014. A PARAFAC-based long-term assessment of DOM in a multi-coagulant drinking water treatment scheme. Environ. Sci. Technol. 48 (3), 1582–1591. https://doi.org/10.1021/es4049384.
- Schmitt-Kopplin, P., Hertkorn, N., Garrison, A.W., Freitag, D., Kettrup, A., 1998.
 Influence of borate buffers on the electrophoretic behavior of humic substances in capillary zone electrophoresis. Anal. Chem. 70 (18), 3798–3808. https://doi.org/10.1021/ac971223j.
- Shukairy, H.M., Miltner, R.J., Summers, R.S., 1994. Bromide's effect on DBP formation, speciation, and control. Part 1, ozonation. J. Am. Water Works Assoc. 86 (6), 72–87. https://doi.org/10.1002/j.1551-8833.1994.tb06211.x.
- Smith, H.G., Sheridan, G.J., Lane, P.N.J., Nyman, P., Haydon, S., 2011. Wildfire effects on water quality in forest catchments: a review with implications for water supply. J. Hydrol. 396 (1–2), 170–192. https://doi.org/10.1016/j.jhydrol.2010.10.043.
- Stewart, K., Dong, A., and Hanigan, D. (n.d.). Reduction of haloacetonitrile-associated risk by adjustment of distribution system pH. ES&T Eng., in Review.
- Summers, R.S., Hooper, S.M., Shukairy, H.M., Solarik, G., Owen, D., 1996. Assessing Dbp Yield: Uniform Formation Conditions. J. Am. Water Works Assoc. 88 (6), 80–93.
- The European Parliament and the Council of the European Union, 2020. Directive (EU) 2020/2184 of the European Parliament and of the Council. Off. J. Eur. Union 2019 (March 2019), 1–62.
- Thurman, E.M., Yu, Y., Ferrer, I., Thorn, K.A., Rosario-Ortiz, F.L., 2020. Molecular identification of water-extractable organic carbon from thermally heated soils: C-13 NMR and accurate mass analyses find benzene and pyridine carboxylic acids. Environ. Sci. Technol. 54 (5), 2994–3001. https://doi.org/10.1021/acs.est.9b05230.
- Tsai, K.P., Uzun, H., Chen, H., Karanfil, T., Chow, A.T., 2019. Control wildfire-induced microcystis aeruginosa blooms by copper sulfate: trade-offs between reducing algal organic matter and promoting disinfection byproduct formation. Water Res. 158, 227–236. https://doi.org/10.1016/j.watres.2019.04.013.
- USEPA, 1995a. Determination of chlorination disinfection by products, chlorinated solvents, and halogenated pesticides/herbicides in drinking water by liquid-liquid extraction and gas chromatography with electron-capture detection.
- USEPA, 1995b. Determination of haloacetic acids and dalapon in drinking water by liquid-liquid extraction, derivatization and gas chromatography with electron capture detection.
- USEPA, 2006. Stage 2 Disinfectants and Disinfection Byproducts Rule (Stage 2 DBPR) 71 FR 388, January 4, 2006, Vol. 71, No. 2.
- Uzun, H., Dahlgren, R.A., Olivares, C., Erdem, C.U., Karanfil, T., Chow, A.T., 2020. Two years of post-wildfire impacts on dissolved organic matter, nitrogen, and precursors of disinfection by-products in California stream waters. Water Res. 181 https://doi. org/10.1016/j.watres.2020.115891.
- Wagner, E.D., Plewa, M.J., 2017. CHO cell cytotoxicity and genotoxicity analyses of disinfection by-products: an updated review. J. Environ. Sci. 58, 64–76. https://doi. org/10.1016/j.jes.2017.04.021.
- Wang, J.J., Dahlgren, R.A., Chow, A.T., 2015. Controlled burning of forest detritus altering spectroscopic characteristics and chlorine reactivity of dissolved organic matter: effects of temperature and oxygen availability. Environ. Sci. Technol. 49 (24), 14019–14027. https://doi.org/10.1021/acs.est.5b03961.
- Wang, J.J., Dahlgren, R.A., Erşan, M.S., Karanfil, T., Chow, A.T., 2016. Temporal variations of disinfection byproduct precursors in wildfire detritus. Water Res. 99, 66–73. https://doi.org/10.1016/j.watres.2016.04.030.
- Weishaar, J.L., Aiken, G.R., Bergamaschi, B.A., Fram, M.S., Fujii, R., Mopper, K., 2003. Evaluation of specific ultraviolet absorbance as an indicator of the chemical composition and reactivity of dissolved organic carbon. Environ. Sci. Technol. 37 (20), 4702–4708. https://doi.org/10.1021/es030360x.
- Westerhoff, P., Mash, H., 2002. Dissolved organic nitrogen in drinking water supplies: a review. J. Water Supply Res. Technol. AQUA 51 (8). https://doi.org/10.2166/ aqua.2002.0038.

- Westerling, A.L., Hidalgo, H.G., Cayan, D.R., Swetnam, T.W., 2006. Warming and earlier spring increase Western U.S. forest wildfire activity. Science 313 (5789), 940–943. https://doi.org/10.1126/science.1128834.
- Writer, J.H., Hohner, A., Oropeza, J., Schmidt, A., Cawley, K., Rosario-Ortiz, F.L., 2014.
 Water treatment implications after the high park wildfire in Colorado. J. Am. Water
 Works Assoc. 106 (4), 85–86. https://doi.org/10.5942/jawwa.2014.106.0055.
- Yan, W., Chen, Y., Han, L., Sun, K., Song, F., Yang, Y., Sun, H., 2022. Pyrogenic dissolved organic matter produced at higher temperature is more photoactive: insight into molecular changes and reactive oxygen species generation. J. Hazard. Mater. 425 (September 2021), 127817 https://doi.org/10.1016/j.jhazmat.2021.127817.